

1 **Elucidation of a potential detection mechanism for high-viscosity solutions in the oral**
2 **cavity using tissue isolation and anatomical characterization**

3 **Brittany L. Miles**

4 **Abstract**

5 Studies on viscosity and its oral perception are limited to relatively thin viscosities
6 ($\eta < 3000\text{cP}$), thinner than many relevant food products. Moreover, multiple modelling studies
7 indicate perception of high-viscosity solutions is linked to filiform papillae deformation, but this
8 has yet to be tested psychophysically. This study sought to characterize the detection mechanism
9 underpinning perception of high-viscosity ($\eta > 3000\text{cP}$) solutions. We hypothesized the tongue
10 would be chiefly responsible for viscosity perception, due to its active role in product
11 manipulation, and that discrimination ability of high-viscosity solutions would be linked to
12 filiform papillary attributes. Just-noticeable difference (JNDs) thresholds for viscosity were
13 determined for participants ($n=59$) using the forced-choice staircase method for
14 glycerin/water/carboxymethyl cellulose solutions ($\eta=4798\text{-}12260\text{cP}$). Participants evaluated
15 solutions by pressing them against the hard palate in “palate-blocked”, “tongue-blocked”, and
16 “unblocked” conditions. Optical profiling was then used to characterize papillary structures in
17 tongue biopsies of a subset of participants ($n=45$). Papillary attributes were related to “palate-
18 blocked” performance using causal analysis. Participants’ differentiations were significantly
19 better ($p < 0.001$, both) using the whole oral cavity ($\text{JND}=1041.71\text{cP} \pm 50.36\text{cP}$) than using tongue
20 ($\text{JND}=1671.26\text{cP} \pm 142.77\text{cP}$) or palate ($\text{JND}=1791.42\text{cP} \pm 117.42\text{cP}$) alone. There was no
21 significant difference between the blocked conditions ($p=0.724$), and performance in those
22 conditions was not significantly correlated ($p=0.773$). “Palate-blocked” data significantly
23 correlated to filiform papillae length and density ($p < 0.001$, and $p=0.005$, respectively). Variation

24 in these attributes alone explained variation in “palate-blocked” JND ($p < 0.001$). Results from
25 psychophysical tests run counter to the original hypothesis, suggesting the tongue and palate play
26 equal roles in viscosity perception, but individuals may differentially utilize these tissues when
27 discriminating between solutions. Similarly, anatomical characterization of filiform papillae
28 provides insight into the role these structures play in high-viscosity perception.

29 **Introduction**

30 Viscosity is a relevant attribute in liquid and semisolid product categories. It has been
31 linked to a variety of textural attributes including positive attributes such as creaminess, and
32 negative attributes such as sliminess and mushiness [1–3]. Yet, the perception of viscosity, like
33 perception of many other textural cues, is not well understood. Oral sensation and perception
34 research has historically focused on the study of chemoception and nociception, with food
35 scientists prioritizing flavor, while dentists and other oral biologists instead concentrate on the
36 study of pain and disease. It is only in the past twenty years that oral somatosensation research
37 and the study of the psychophysiology of texture perception have begun to consistently grow and
38 diversify beyond product specific applications. Companies and scientists are now trying to
39 understand how people interact with their food, why they choose the products they do, and more
40 importantly here, what systems, structures, and underlying processing mechanisms might be
41 driving product-related decisions.

42 Some preliminary work has been done to characterize oral viscosity perception in
43 humans. These studies can be broken into two main categories: those focused on determining the
44 power function relating physical increases in viscosity to perceived increases in thickness [4–6]
45 and those comparing oral viscosity evaluation to other evaluation methods (i.e. stirring, pouring,
46 etc.) [2,7]. Rarely did studies focus on the mechanisms driving viscosity perception, or how

47 individual variation may be impacting the process. However, more recently, mathematical
48 modeling studies have investigated a potential mechanism involved in oral viscosity perception,
49 the directional deformation of the filiform papillae. First proposed by van Aken (2010) and
50 further investigated by Lauga, Pipe, and Révérend (2016), these studies suggest the idea of
51 filiform papillae as strain amplifiers on the tongue capable of interacting with viscous solutions
52 on the tongue's surface [8,9]. The structures may be of such importance that their presence
53 causes an increase of strain in response to viscous solution by an order of magnitude [9]. This
54 directional deformation is postulated to then transduce a signal to the brain either via specialized
55 mechanoreceptors inside the papilla structure or via a sublingual receptor responding to strain on
56 the surface [8–10].

57 Filiform papillae are the non-tasting papillae that cover the majority of the front two-third
58 of the human tongue. They are comprised of cornified projections made of keratin [11]. While
59 these cells do undergo keratin-type differentiation, they do not harden but instead squamatize and
60 plaque on the surface of the structure, leading to a roughened appearance. The structures
61 themselves are a complex, comprised of up to 30 hair-like projections off of one papillary body,
62 although the body and hairs are thought to act as a single unit [11–13]. They have been proposed
63 to play a variety of roles from helping to aid in bolus formation and swallowing to providing
64 optimal salivary wetting of the tongue [10]. Unfortunately, while studies appear to be in
65 agreement about the general structural layout on the tongue, reports of the papillae's length
66 (anywhere from 250 μ m to 2-3mm), width (100 μ m to over 450 μ m), and assumptions on their
67 elasticity (2.6-25kPa) vary greatly [8–10,12,13]. This in turn leads to multiple proposed viscosity
68 cut-offs for when these structures may become relevant for perception. For thinner solutions
69 ($\eta < 100$), it is universally accepted the structures are likely irrelevant. These solutions do not

70 generate enough force to lead to deformation. With such variations in proposed structure,
71 however, there is not agreement as to what exact minimum viscosity leads to deformation. Most
72 conservatively, van Aken (2010) proposed that a minimum viscosity of 1000cP was needed. As
73 the authors were unable to find a conclusive set of average dimensions prior to the study, this
74 more stringent cutoff was used to ensure all solutions could be evaluated via the proposed
75 papillary deformation mechanism.

76 Unfortunately, the bulk of the solutions evaluated in the psychophysical studies on
77 viscosity mentioned previously fall below the 1000cP cutoff [2,4–7,14]. Assuming these
78 solutions could potentially be being detected via a different mechanism or pathway, the findings
79 from these studies have limited applicability here. Moreover, of the limited studies that do exist
80 with solutions in the higher-viscosity range, they tend to utilize confounded systems such as
81 sucrose syrups, which can be also identified on the basis sweetness [4]. Additionally, the primary
82 method used in these studies, magnitude estimation, is prone to memory effects leading to
83 participants comparing the tested solutions to the previous sample instead of the reference unless
84 frequent representation of the reference occurs[2,4,6]. Thus, we elected to utilize the forced-
85 choice, staircase method, which presents the reference as part of every comparison, with the aim
86 of limiting memory effects here.

87 Fortunately, extensive work has been done to characterize the mechanical evaluation
88 process of high-viscosity fluids in the oral cavity. In a seminal study by Shama and Sherman
89 (1973) researchers characterized the average shear rate utilized by participants to evaluate a
90 series of different liquid food items ranging from water to glucose syrup. Solutions in the high-
91 viscosity range, were consistently evaluated at shear rates between 10 s^{-1} and 50 s^{-1} [3]. Further
92 studies have concentrated of the evaluation of these high-viscosity solutions, and data suggests

93 that the evaluation rate is likely toward the lower end of the reported values, near 10 s^{-1} [15].
94 Thus, it can be assumed that for any stimuli used here, the solutions should be devoid of any
95 taste or aroma cues that might aid in identification, and recorded viscosity should be above
96 1000cP over the $10\text{-}50\text{s}^{-1}$ range.

97 Another challenge that has likely limited previous evaluation of filiform papillae in
98 somatosensation is their small size, which can make them challenging to visualize completely. In
99 order to identify structural variance in the population to relate it to performance, it was necessary
100 to find a method for characterizing filiform papillae in humans. While the non-invasive Denver
101 Papillae Protocol is often used to quantify fungiform papillae size and density, the method lacks
102 the consistency and detail necessary for quantifying variations in attributes of the filiform
103 papillae such as average papilla height, width, and curvature [16]. Moreover, utilizing a hand
104 microscope for *in vivo* visualization of the structures was also challenging due to difficulty
105 completely immobilizing the tongue to allow for focusing. While the very accurate scanning
106 electron microscopy (SEM) has been successfully used to accurately characterize variation in
107 papillae previously, this method is time consuming, requiring a minimum of 48 hour to prep
108 tissue, and can be destructive[13,17,18]. Instead, a novel method for the evaluation of papillary
109 variance, optical profilometry using a Keyence VK-X microscope (KEYENCE, Osaka, Japan),
110 was utilized.

111 Optical profilometry is a two-part process during which a laser scans the surface of an
112 object, analyzing the distance from the source. This data is then overlaid on a picture of the
113 surface, generating a visual “roughness profile” for each sample, as well as a height heat map.
114 This data is then integrated into a three-dimensional model of the surface. The microscope
115 possesses nanometer level resolution and produces images of similar quality to those seen in

116 SEM. Unlike SEM, however, optical profilometry requires minimal prep, without complete
117 desiccation required. This process allowed for faster visualization without tissue loss. Once
118 characterized, anatomical variation could be related to psychophysical ability, providing a
119 concrete way to investigate the role of the filiform papillae in viscosity perception.

120 Taking this information together, we arrive at two primary objectives for this study. First,
121 characterize the perception of high-viscosity solutions in the oral cavity via psychophysical
122 testing. Utilizing tissue isolation, the relative contributions of both the tongue and the palate can
123 be assessed. Second, determine what role, if any, the filiform papillae may be playing in
124 viscosity perception. By correlating papillary traits to psychophysical performance, we can
125 assess not only the role the structures may generally play, but also how individual variation in
126 these structures may influence viscosity perception. We hypothesize that the tongue will show a
127 greater acuity for viscosity perception due to its role in product manipulation and possession of
128 papillary strain amplifiers, and that the perception of viscosity on the tongue will be related to
129 the filiform papillary attributes of length, width, and density.

130 **Methods**

131 *Subjects*

132 59 participants (age 19-40, 18M/41F) were recruited via the Ohio State University
133 Consumer Sensory Database. Individuals completed a pre-test screener (Qualtrics, Provo, UT)
134 including questions on age, physical limitations or back problems, food allergies or sensitivities,
135 smoking status, presence of oral diseases, and willingness to undergo the biopsy procedure. As
136 with previous studies in this lab, the age range for recruitment was restricted to the ages of 18-40
137 to limit any potential decreases in acuity attributable to age [19,20]. Individuals with a self-

138 reported history of an oral disease or condition, food allergies or sensitives, back or mobility
139 problems that would prevent them from transferring to the dental chair or completing the
140 physical task, as well as smokers, were excluded. Subjects were instructed not to eat food or
141 drink anything other than water one hour prior to their testing sessions. Each subject completed
142 the psychophysical testing individually during two, 1-hour sessions one week apart. After
143 completion of psychophysical testing, subjects underwent the biopsy protocol. All biopsies were
144 completed on the same day of the week in batches of 15 by a practicing oral surgeon. Biopsies
145 were taken between 4-14 days after the last psychophysical testing session. Subjects were
146 compensated \$70 for their participation in the study, \$20 after each of the psychophysical
147 sessions, and \$30 following completion of the biopsy procedure. All parts of this study were
148 approved by the Ohio State University Instructional Review Board (2013B0277, psychophysical
149 protocol and 2018H0509, biopsy protocol). Data was collected under the written and informed
150 consent of each subject.

151 *Viscosity Discrimination*

152 Viscosity discrimination ability for high-viscosity solutions in the oral cavity was
153 determined using the forced-choice, up-down staircase method to assess participants' Just-
154 Noticeable-Difference (JND) threshold for viscosity [21,22]. As previously stated, "high-
155 viscosity" solutions are typically evaluated in the mouth at a shear rate between 10-50s⁻¹ [3].
156 Thus, stimuli were developed that had apparent viscosities above 1000cP across this range of
157 shear rates when measured with a parallel plate rheometer (Anton Paar, Graz, Austria). Stimuli
158 consisted of nine glycerol/water/carboxymethyl cellulose (CMC) solutions, one reference
159 solution ([CMC]=1.125% w/v, $\bar{\eta}$ =5068cP \pm 270cP) and eight variable solutions ([CMC] =
160 1.1538%-1.5% w/v, $\bar{\eta}$ =5507cP-11840cP \pm 321cP). Variable solutions increased in concentration

161 of CMC in 0.03125% w/v increments. All solutions were made with a 55:45 reverse osmosis
162 (RO) water/glycerol solution. Glycerol (Essential Depot, Inc., Sebring, FL) was utilized in this
163 mixture due to its known synergistic thickening with CMC (Sigma-Aldrich Corp., St. Louis,
164 MO) [23]. Solutions were stored in sealed, plastic containers at ambient temperature (20-23°C)
165 before being portioned out into 10mL slip-tip syringes outfitted with 2cm of flexible, plastic
166 tubing, for the duration of testing.

167 Viscosity discrimination ability was evaluated in three different blocking conditions: an
168 Unblocked (UB) condition wherein individuals evaluated solutions using their entire oral cavity,
169 a Palate-Blocked (PB) condition wherein individuals evaluated solutions with only their tongue
170 while wearing a custom-molded mouth piece to block their hard palate (Figure 1A and B), and a
171 Tongue-Blocked (TB) condition wherein individuals evaluated solutions using only the surface
172 of their palate while wearing a flexible, silicone mouthpiece to block the tongue's surface
173 (Figure 1C and D). Physical barriers, as opposed to topical numbing agents, were used due to the
174 challenges of achieving complete numbing seen previously [24]. Two of these evaluations would
175 occur during one of the two sessions, while one evaluation was completed during the other
176 session. The order of these conditions and number of conditions per session was randomized and
177 counterbalanced across participants.

178 During the first psychophysical session, participants would complete the informed
179 consent and a brief demographic questionnaire before molding their PB mouthpiece (Figure 1A
180 and B). The mouthpiece was created by pouring 71°C water over 30mL of InstaMorph moldable
181 plastic beads (Happy Wire Dog, LLC, Scottsdale, AZ) and allowing the beads to sit for 105
182 seconds. The beads were then removed from the water by the researcher and squeezed to remove
183 any remaining liquid. The participant was instructed to bite down into the plastic and spread it

184 across the palate using their thumbs, making sure to cover the palate completely, until at least the
185 third set of molars. Upon completion, the mouthpiece visually inspected by the researcher to
186 ensure suitable coverage from the piece, and the mouthpiece was then placed into ambient
187 temperature water until it became opaque, indicating the mouthpiece had hardened. Once
188 hardened, the participant would test fit the mouthpiece again for comfort and to ensure that the
189 piece did not cause gagging. In the event the piece was uncomfortable, it would be remolded
190 using the same procedure as above.

191 TB mouthpieces were cut from 1mm thick silicone baking sheet (Figure 1C and D). The
192 mouth pieces consisted of a rounded portion that was inserted into the mouth to cover the tongue,
193 as well as two “handles”, extra pieces of mat that would sit against either cheek for the
194 participant to grasp (Figure 1C). Participants held the handles during the evaluation and pulled
195 slightly outward to prevent the mouthpiece from sliding during the evaluation (Figure 1D).
196 Mouthpieces were available in two sizes that varied in the width of the insertable section. Based
197 on visual assessment, researchers would provide participants with a mouthpiece of a given size.
198 In the event the mouthpiece was uncomfortable or did not completely cover the front 2/3 of the
199 tongue, the other size was used.

200 As the final step before both testing sessions, participants would rinse with a concentrated
201 Gymnema leaf extract solution (Bio-Botanica, Inc., Hauppauge, NY) made with 2mL of extract
202 (~1200mg of gymnemic acid) and 6mL of RO water for one minute before expectorating the
203 solution. Gymnemic acids from the Gymnema plant have been shown to inhibit the perception of
204 sweetness by binding to taste cells involved in sweetness perception [25]. This rinse was done to
205 help block any sweetness coming from the glycerol in the test solutions. While the solutions
206 should be iso-intense in terms of sweetness (as all solutions contained the same proportion of

207 glycerol to water), rinsing helped to guarantee that the only perceivable difference between the
208 solutions was viscosity.

209 Once blocking was completed participants were seated in a dental chair and reclined to
210 allow researchers access to the oral cavity. A trashcan was placed between the participant's
211 knees, ensuring that one leg was in contact with the edge of the container. Participants were then
212 instructed on the evaluation procedure and allowed to ask questions if they had any. They were
213 provided with paper towel to clean their hands and the mouthpiece while testing before being
214 blindfolded to prevent solution discrimination based on visual cues. During the study,
215 participants evaluated pairs of solutions one of which was always the reference solution ($\bar{\eta}$
216 =5068cP \pm 270cP), and another, variable solution. One at a time, 0.5mL of the solution was
217 applied to the dorsal medial tongue. Once the solution was fully applied, the researcher would
218 give a verbal signal, and the participant would press the applied solution against the rugae of the
219 palate three times before the solution was removed by the participant using a KimWipe
220 (Kimberly-Clark, Irving, TX). In the event there was any residual solution, more wipes were
221 provided as needed. KimWipes were disposed of in the provided trashcan. The short, three-press
222 evaluation was chosen to help standardize oral movement during evaluation and limit salivary
223 incorporation. Wiping was used instead of expectorating or swallow to help minimize cues
224 coming from the lips or esophagus, respectively. The hands, particularly with the KimWipe
225 buffer were thought to be less sensitive than either of these tissues [2].

226 Once the first solution was removed, the second solution was applied in a similar fashion.
227 However, before participants removed solution two from the mouth, they were asked to provide
228 an answer – either one or two – as to which solution they felt was thicker. If they felt the
229 solutions were of equal thickness, they were informed that they would still need to choose one of

230 the two solutions. In the event they chose the thicker solution, the variable solution in the next
231 trial decreased in viscosity, becoming closer to the reference solution. If they chose the thinner
232 solution, the two solutions got farther apart. This process was repeated until eight reversals were
233 achieved. A reversal consisted of a change in the participant's direction on the staircase, either an
234 incorrect response followed by a correct response or a correct response followed by an incorrect
235 one. In the event a participant correctly identified the thinnest variable solution (ceiling) or
236 incorrectly identified the thickest one (floor) this was also counted as a reversal as no thinner or
237 thicker solutions were available. In the trials following these events, participants would be
238 presented with the same comparison as in the previous trial. Average JND was calculated by
239 subtracting the apparent viscosity of the reference solution ($\bar{\eta} = 5068\text{cP} \pm 270\text{cP}$) from each of the
240 reversals and averaging the resulting values. Solution presentation order was randomized and
241 counterbalanced across the trials.

242 In sessions with two evaluation conditions, participants were given the option to take a
243 brief break (< 2min) before returning to the chair for the second condition. The participants also
244 completed a 30s maintenance rinse using the gymnemic acid solution as needed. In the blocked
245 evaluation conditions the evaluation protocol was the same as in the UB condition, however,
246 participants were instructed to either press the solutions against the plastic mouthpiece in the PB
247 condition, or to press the silicone mouthpiece (which the solution was applied to) against the
248 palate in the TB condition. In the PB trials, participants were instructed to wear the mouthpieces
249 continuously during each paired comparison, wiping the mouthpiece and oral cavity between
250 trials, while in the TB trials participants were allowed to remove the mouthpiece for cleaning
251 between solutions. This decision was made due to the difficulty some participants had removing

252 the PB mouthpieces, which was viewed as a potential distractor if done between compared
253 solutions.

254 *Lingual Biopsy*

255 Biopsies were completed in the Department of Oral and Maxillofacial Surgery at the
256 Ohio State University's College of Dentistry by a trained oral surgeon. After obtaining surgical
257 consent and acceptable vital signs, participants' tongues were isolated and retracted by a surgical
258 assistant while local anesthesia was administered by the surgeon. 1.8ml of 2% lidocaine with
259 1:100,000 epinephrine was locally infiltrated at the surgical site. After 5 minutes had passed and
260 vasoconstriction was visualized, the tongue was again isolated and retracted for the biopsy
261 procedure. A 5mm biopsy punch (Figure 2) was used to incise through mucosa and submucosa
262 in the middle third of the dorsal tongue to the right of the midline, and tissue was removed using
263 forceps (Figure 2). Once removed the biopsied tissue was placed in a neutral phosphate-buffered
264 20% formalin solution at 20°C and sealed while the wound was closed. The samples were then
265 stored in the fixing solution at 4°C for one week, prior to anatomical characterization.

266 *Anatomical Characterization*

267 Anatomical characterization was completed for a subset of participants (n=45) using
268 optical profiling (Figure 2). Only a subset of participants were analyzed either due to a failure to
269 attend the biopsy session (n=4), or due to blood present on the surface of the sample during
270 fixing (n=11) preventing the surface structures from being sufficiently visualized. For this study,
271 a Keyence VK-X250 (Keyence Corporation, Itasca, IL) 3D laser scanning microscope was used.
272 Biopsied samples were removed from the fixative, rinsed with DI water, and placed on a
273 disposable, glass microscope slide for the evaluation. The slide was placed on the stage of the

274 analyzer with the papillae oriented toward the top of the stage when possible. Eight images were
275 taken using the associated imaging software from across the sample using 10x optical zoom,
276 being careful to minimize overlap between the images. While the majority of the samples
277 contained only filiform papillae, a small subset of the samples (n=5) did have at least one
278 fungiform papilla present. To ensure accurate density measurements, all images taken excluded
279 these structures. Following imaging, samples were placed in cryoprotectant (glucose and 1%
280 Phosphate-Buffered Saline) and stored at -80°C.

281 Papillary data was analyzed using Keyence Multifile Analyzer software (Keyence
282 Corporation, Itasca, IL). Prior to measuring, all samples were corrected for any surface tilt or
283 general curvature. Papillary length was determined using the profile tool to draw segments from
284 the base to tip of papillae, parallel to the direction of the papillary body using either the 2pt line
285 tool or circle tool (Figure 2A and D). Curves were then smoothed by average weight to
286 minimize noise in the curve coming from the papillary surface. Finally, the Continuous Segment
287 (CS) length tool was used to measure the length of the curve, measuring from the local minimum
288 at the base of the papilla to the inflection point at the tip (Figure 2D). As papillae are not flat
289 structures, taking the segment length (as opposed to the absolute distance along the X and Y
290 planes), factored in distance in the Z plane. Papillary width was measured similarly, drawing a
291 2pt segment perpendicular to the base of the papillae inside the interpapillary furrow (Figure 2B
292 and E). However, as diameter did not depend on the surface profile, width was quantified using
293 the 2pt segment tool, measuring at the inflection point on either side of the papilla (Figure 2E).
294 Three length and width measurements were taken per image.

295 Papillary density was calculated by visually identifying the number of papillae present in
296 an image (Figure 2C and F). Papillae were considered separate if there was a clearly identifiable

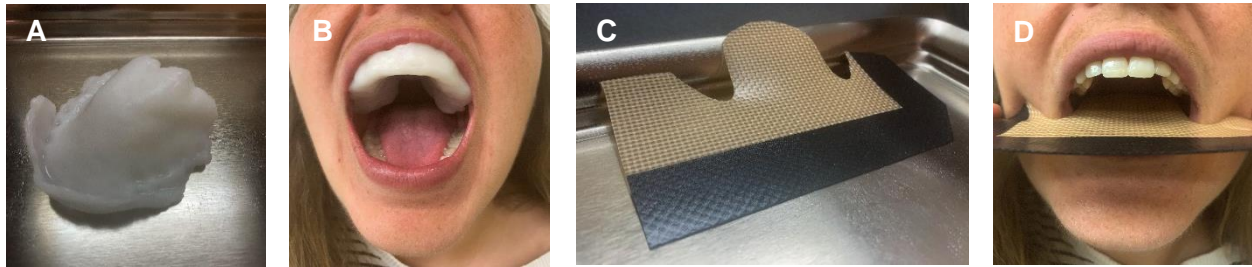
297 base wherein hair structures attached or if structures were clearly separated by an interpapillary
298 furrow. Using the plane tool, count data was collected, marking each papilla with an x to prevent
299 double counting. In the event there was an incomplete papilla, the structure was only counted if
300 the base was in the frame. In the event only the hair structures were present, the papilla was not
301 counted. Density was determined by dividing the count data by the area as calculated by the XY-
302 measure function (Figure 2F).

303 *Data Analysis*

304 Average viscosity JND was analyzed using a one-way analysis of variance (ANOVA) in
305 SPSS Statistical Analysis Software (IBM, Armonk, NY) with JND as the dependent factor and a
306 Tukey post-hoc to determine if any of the blocking conditions showed a significant difference in
307 acuity ($\alpha=0.05$). Blocking condition and participant were used as the main effects. To analyze
308 papillary data, values were averaged across images to determine an average papillary length,
309 width, and density for each individual. Papillary attributes were then correlated to PB JND using
310 a linear correlation ($\alpha=0.05$). Additionally, causal analysis was run using the linear regression
311 tool to determine the impact of the average measured papillary attributes of length, width, and
312 density, as well as demographic information including age and gender. The model was executed
313 in a stepwise fashion, removing attributes that did not meet the criteria for inclusion ($p \geq 0.100$).

314

315



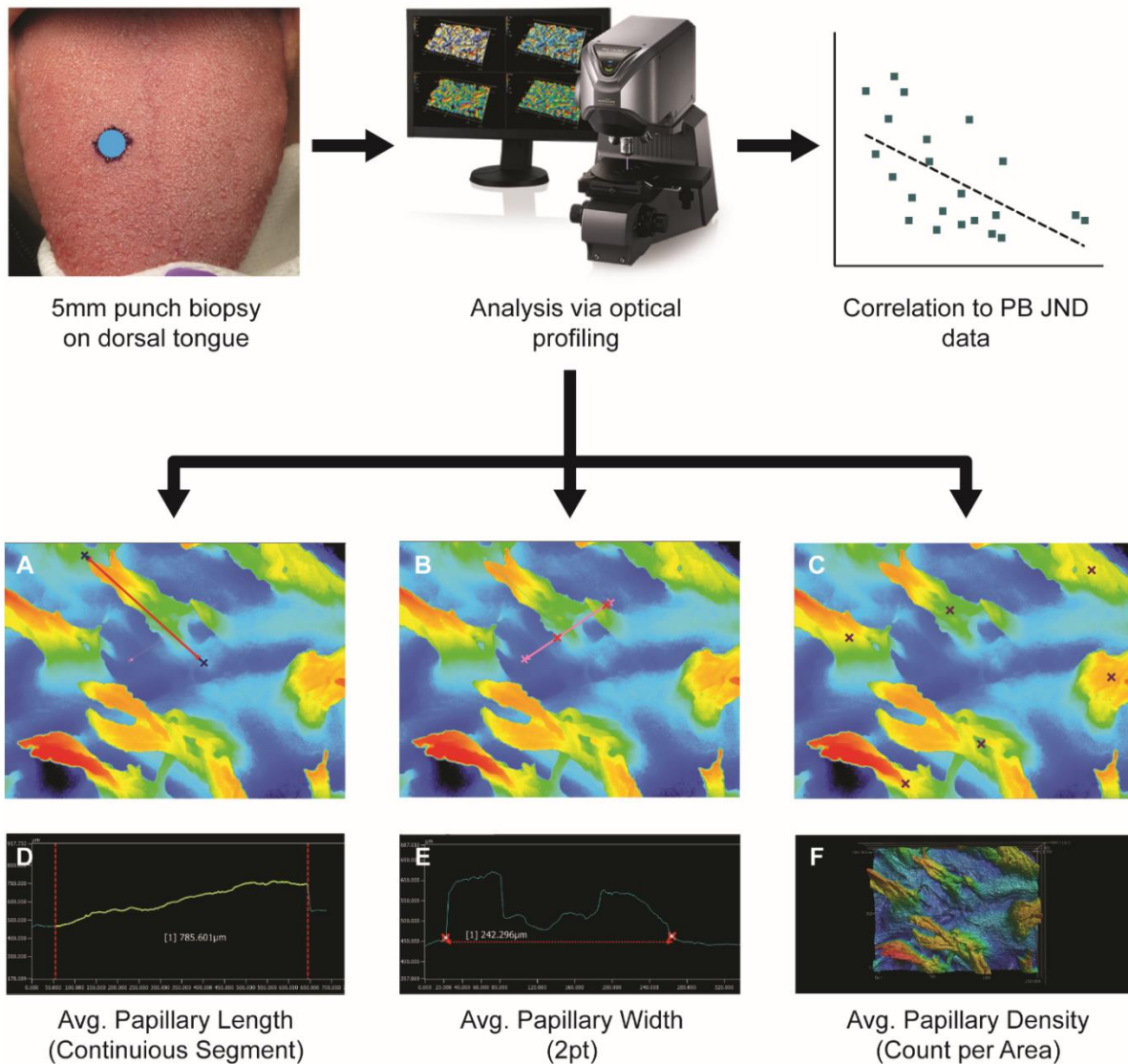
316 Palate-Blocked Mouthpiece

Tongue-Blocked Mouthpiece

317

Figure 1: Example mouthpieces for the Palate-Blocked (PB) and Tongue-Blocked (TB)

evaluation conditions. PB mouthpieces were made of InstaMorph moldable plastic and custom-molded to the participants' oral cavity prior to testing (A and B). All mouthpieces covered the hard palate past at least the third molar. TB mouthpieces were cut from a reusable silicone baking sheet (C and D). Mouthpieces were available in "Large" and "Small" sizes, and sizing was determined by visually ensuring adequate tongue coverage while maintaining participant comfort.



319

320 **Figure 2A-F: Technique for biopsy analysis via optical profiling.** Samples were obtained via a

321 5mm punch biopsy of the medial, dorsal tongue epithelium adjacent to the midline and fixed in

322 20% formalin for one week at 4°C. Samples were then analyzed using optical profiling to obtain

323 three-dimensional surface models of the tongue surface. Eight images were taken per sample at

324 10x optical zoom (example images: A-C). Average papillary length was determined using the

325 continuous segment tool (A and D), measuring for the local minimum at the base of the papillae

326 to the inflection point, where a sudden drop in height was noted. Average papillary width was

327 determined using the two-point distance tool to calculate the separation between the inflection
328 points on either side of the base of the papillae (B and D). Length and width measurements were
329 taken in triplicate on each image for all eight images and the mathematical average was taken to
330 determine the average length and width for each individual. Average papillary density was
331 measured using the count tool to count the papillae in each image. Partial papillae were included
332 only if the papillary base was visible in the image. Area was standardized across counts and then
333 the mathematical average was taken across images to determine an individual's average density.
334 Average values from all three measurements were then correlated to PB JND data to determine
335 relation.

336 **Results**

337 *Viscosity Discrimination*

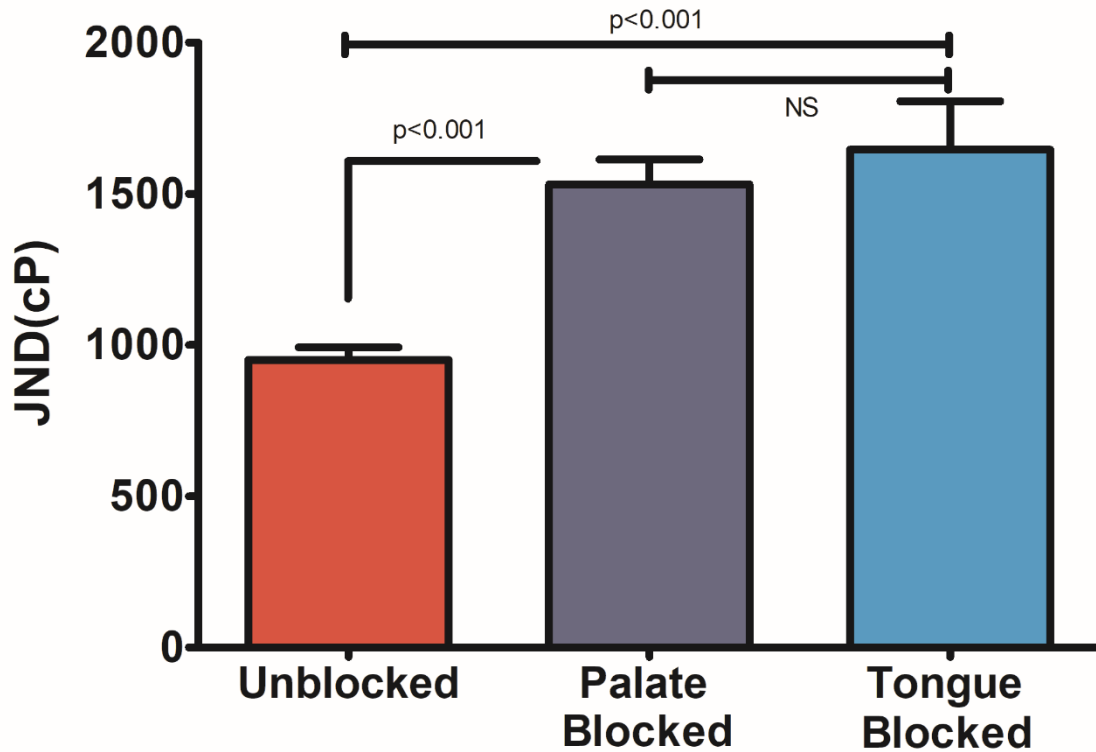
338 There was a significant difference found between the JNDs in viscosity for the different
339 psychophysical conditions ($F= 13.521$, $p<0.001$). On average, individuals' UB JNDs ($\overline{\Delta\eta} =$
340 $1041.71\text{cP} \pm 50.36\text{cP}$) were significantly lower ($p<0.001$, both) than their JNDs in the PB ($\overline{\Delta\eta} =$
341 $1671.26\text{cP} \pm 142.77\text{cP}$) or TB ($\overline{\Delta\eta} = 1791.42\text{cP} \pm 117.42\text{cP}$) conditions; however, there was no
342 significant difference between the JNDs in the blocked treatments ($p=0.724$, Figure 3).
343 Additionally, there was no significant correlation ($R^2=0.0014$, $p=0.773$) between performance in
344 the PB and TB conditions. That is to say that just because an individual was sensitive to
345 differences in viscosity with one tissue did not necessarily mean they were sensitive to
346 differences with the other. These findings are not in agreement with the initial hypothesis that the
347 tongue would be chiefly responsible for viscosity perception in the oral cavity and instead
348 suggest a larger contribution from the hard palate than first postulated.

349 *Anatomical Characterization*

350 Characterization of filiform papillary length, width, and density indicated a greater
351 diversity in size and shape than originally anticipated (Figure 4A-D, Figure 5A-C). While
352 average papillary length was $774.74\mu\text{m} \pm 29.15\mu\text{m}$, values ranged from $462.94\mu\text{m}$ to $1177.21\mu\text{m}$
353 with four individuals with averages below $500\mu\text{m}$ and four individuals with values over $1100\mu\text{m}$.
354 Average length did not correlate with average width ($R^2= 0.017$, $p=0.385$) or average density
355 ($R^2=0.012$, $p=0.469$), however the two categories were slightly related ($R^2= 0.089$, $p=0.047$).
356 When correlated to PB JND, significant relationships were seen between length and PB JND
357 ($R^2=0.337$, $p<0.001$) and density and PB JND ($R^2=0.178$, $p=0.005$) (Figure 6A and B). There
358 was an inverse relationship present for both attributes with individuals with more, longer,
359 papillae showing lower JNDs, translating to a higher acuity. Width was not significantly
360 correlated to psychophysical performance ($R^2=0.001$, $p=0.996$) (Figure 6C).

361 Further investigation via causal analysis indicated that the significant filiform papillary
362 attributes of length and density were not only strongly correlated to PB JND, but also had a
363 causal relationship with an individual's acuity (Adj. $R^2=0.412$, $p<0.001$, Table 1). Papillary
364 length appeared to play the most significant role in predicting an individual's PB JND ($\beta= -$
365 0.496 , $p<0.001$), while density was also highly significant ($\beta= -0.385$, $p=0.004$). The other
366 attributes tested in the model, papillary width, age, and gender, were not found to be significant.
367 Moreover, when all non-significant terms were removed, there was an increase in model-fit (Adj.
368 $R^2=0.431$, $p<0.001$), the highest of any of any of the models built using the five terms. Data here
369 are in agreement with the second hypothesis, suggesting viscosity perception on the tongue is
370 significantly related to filiform papillary attributes.

371



372

373 **Figure 3: Average Viscosity JNDs for the oral cavity and isolated tissues.** Just-Noticeable-

374 Difference (JND) thresholds were calculated by subtracting the apparent viscosity of the

375 reference stimuli from each of the eight reversals and then taking the mathematical average of

376 those values. Values were compared using a one-way ANOVA with JND as the dependent

377 variable ($\alpha=0.05$, Tukey post-hoc). Individuals were significantly better ($p<0.001$, both) at

378 discriminating between viscosities with both tissues than in either blocked condition, but there

379 was no significant difference between the two blocked conditions ($p=0.724$). Error bars represent

380 standard error of the mean.

381

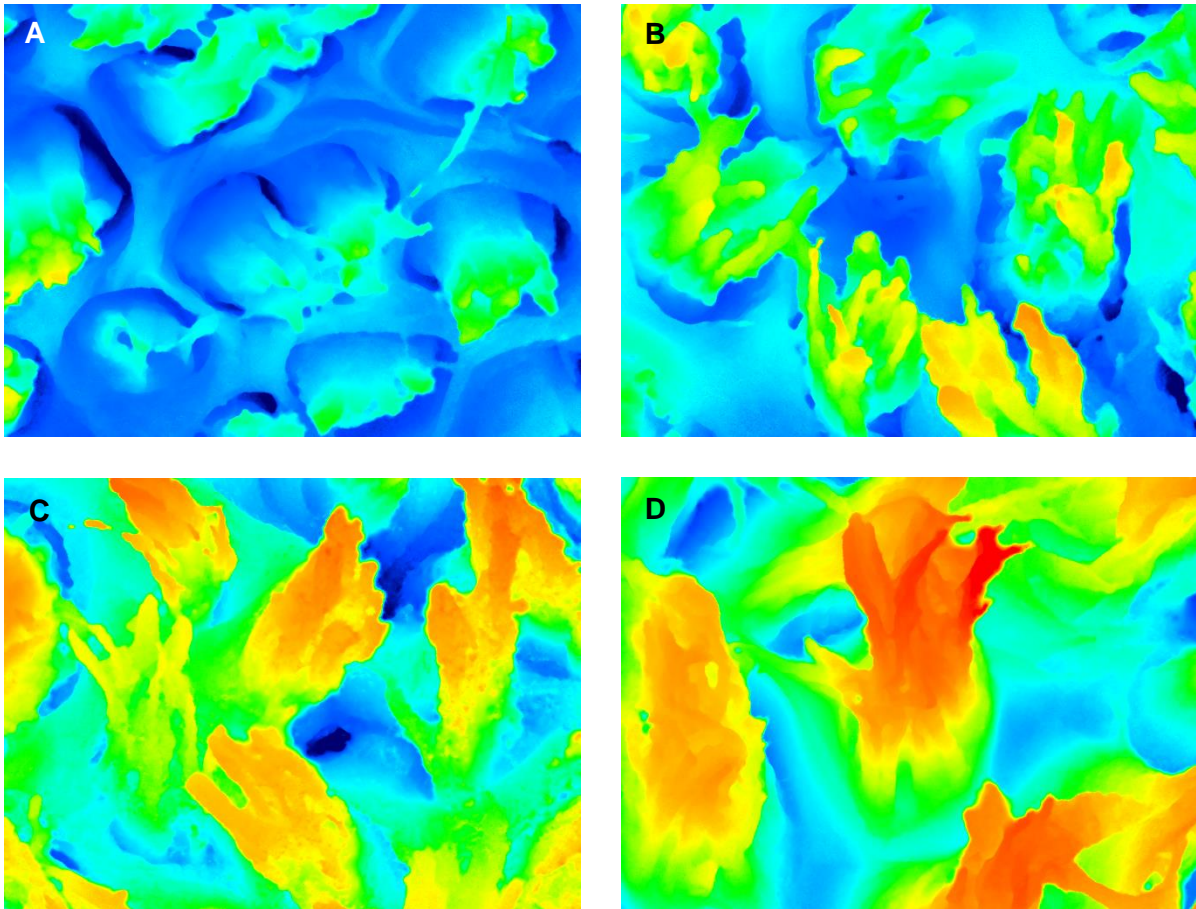


Figure 4(A-D): Visualization of representative papillary length variation across participants. Images include height heat maps from the participants with the shortest papillae (A, $\bar{h}=462.95\mu\text{m}$), the longest papillae (D, $\bar{h}=1177.21\mu\text{m}$), and representative samples participants from the lower and upper quartiles (B, $\bar{h}=546.24\mu\text{m}$ and C, $\bar{h}=818.71\mu\text{m}$, respectively). Above images standardized to uniform height scale ranging from dark blue to red for clarity ($89.359\mu\text{m}$ - $1086.593\mu\text{m}$).

382

383

384

385

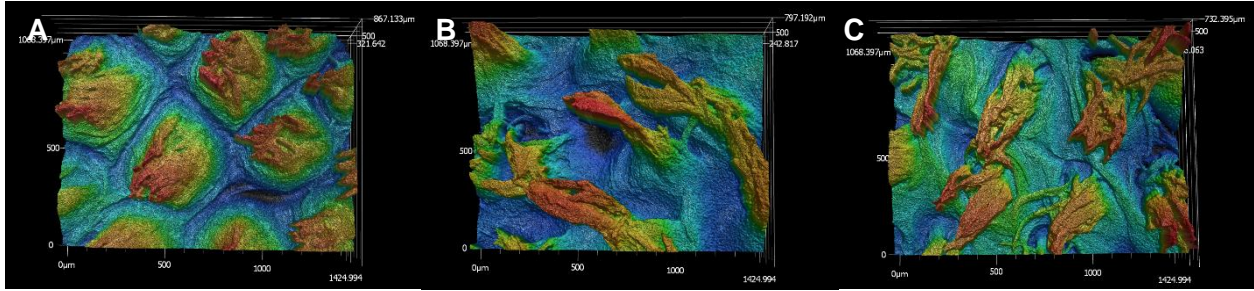
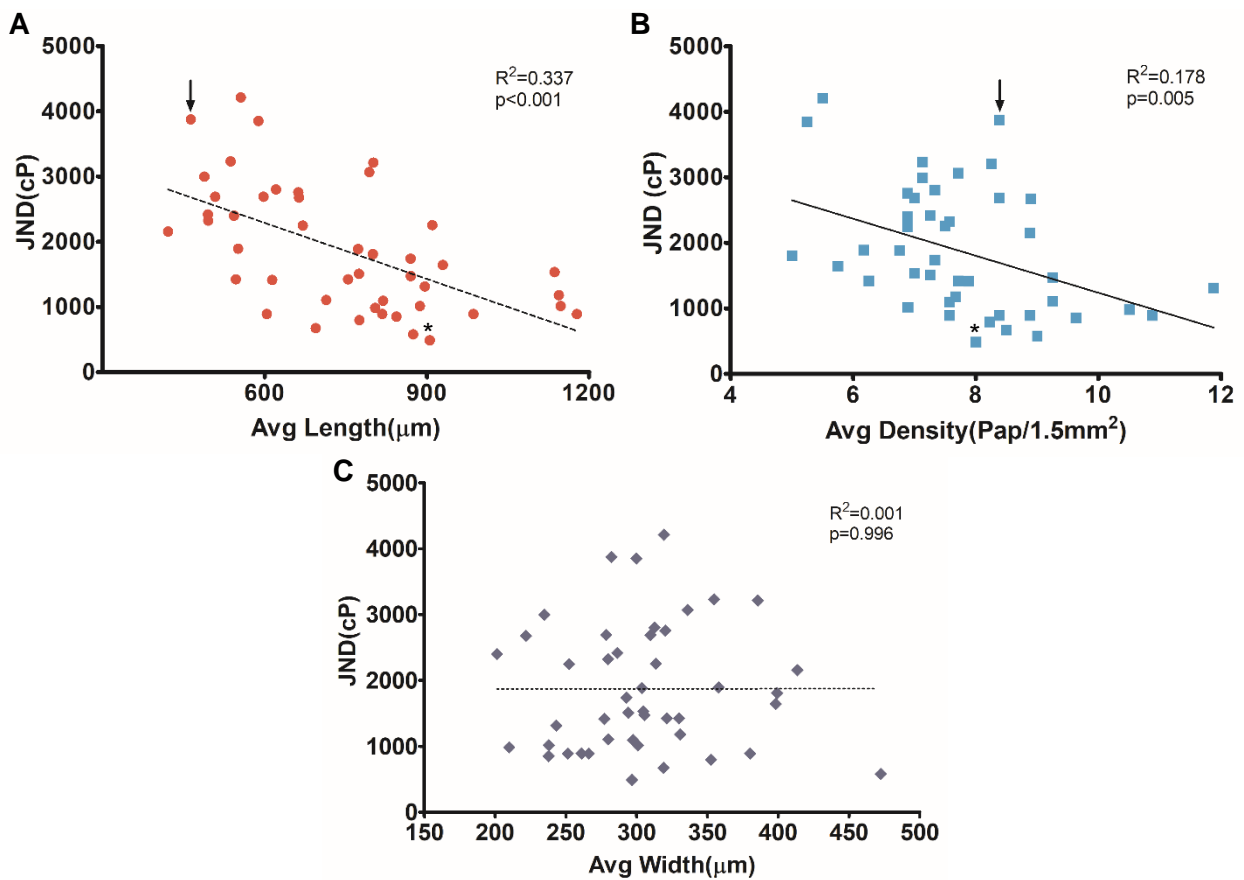


Figure 5A-C: Surface models of tongues of individuals with equivalent PB JNDs. While pictured individuals show a high degree of diversity in structure shape, length, and density all individuals show a similar and high level of acuity (Avg. JND = 714.95cP±158.75cP). Multiple different phenotypes appear to be equally as successful at discriminating between high-viscosity fluids.

386

387



388 **Figure 6A-C: Linear correlations of key papillary attributes and average Palate-Blocked**
 389 **JND.** Palate-blocked JND was correlated to papillary attributes of length, width, and density
 390 using a linear correlation. Average papillary length and density were significantly correlated to
 391 JND ($p < 0.001$ and $p = 0.005$, A&B, respectively), but papillary width showed no significant
 392 correlation ($p = 0.996$, C). Arrow (\downarrow) in A and B denotes the same subject, relevant for much
 393 higher JND than estimated by density. Asterisk (*) in A and B denotes the same subject, relevant
 394 for much lower JND than estimated by density.

394 **Table 1: Causal analysis of variation in Palate-Blocked JND.** A linear regression was
 395 completed utilizing all collected variables to assess their relative contributions to variation in PB
 396 JND. The proposed model was highly significant ($p < 0.001$). Average papillary length and
 397 papillary density were both significant drivers of variation ($p < 0.001$ and $p = 0.004$, respectively).
 398 Average papillary width, age, and gender were not significant.

Model*	Unstandardized Coefficients		Standardized Coefficients	t	p-value
	B	Std. Error	β		
(Constant)	6963.216	1532.168		4.545	<0.001
Pap. Length	-2.447	0.605	-0.496	-4.043	<0.001
Pap. Density	-266.673	86.158	-0.385	-3.095	0.004
Pap. Width	-0.704	2.172	0.041	-0.324	0.748
Age	-17.573	27.462	-0.083	-0.640	0.526
Gender	-325.515	264.949	-0.163	-1.229	0.227

* $p < 0.001$, Adj. $R^2 = 0.412$

399

400 Discussion

401 *Viscosity Discrimination*

402 Based on the JNDs of the three psychophysical conditions it becomes immediately clear
 403 that the tongue is not the sole or even the main structure involved in viscosity perception in the

404 mouth (Figure 3). Instead, it appears that, on average, the tongue and palate may play an equal
405 role in viscosity perception. At the individual level, however, the lack of correlation between the
406 TB and PB JNDs, as well as a lack of any correlation of the blocking conditions to each other
407 suggests that there may be multiple, different, tissue-specific mechanisms at play. This may
408 allow individuals to compensate for a lack of sensitivity of one tissue with sensitivity of the
409 other. Only in the blocked conditions, wherein the compensatory or insensitive tissue is removed,
410 can a structure-specific mechanism be evaluated. A similar phenomenon has been observed
411 when assessing size using these tissues. Engelen, et al. (2002) found that the palate hindered the
412 estimation of the size of large (4-9mm) spheres (attributed to a limited contact area between the
413 sphere and the hard palate) when compared to evaluation with the tongue alone [26]. This
414 finding further underscored the decision to compare papillary traits to the PB JND values, not
415 UB JND ones. Additionally, it is challenging to compare JND values obtained here to values
416 reported previously for two reasons. First, most reported values have been obtained via
417 magnitude estimation, not paired comparison, and second with such low viscosities used in other
418 studies, it is unlikely that the perceptual mechanism proposed here is being utilized. Thus, the
419 psychophysical curves generated in previous studies likely do not apply here.

420 The relatively equivalent contribution from the palate also highlights an important area
421 for future study. Immunohistochemical studies in rats found that the palatal rugae are innervated
422 with both Merkel discs (SAI) and Messier corpuscles (RAI), two kinds of specialized,
423 mechanoreceptive nerve endings [27]. While similar innervation studies have not been carried
424 out in human palatal tissue, it is possible the equivalent structures are similarly innervated. Thus,
425 a future study into what drives viscosity perception on the palate focusing on the rugae, similar
426 to the one undertaken here on the filiform papillae on the tongue, could provide insight into

427 another mechanism of oral viscosity perception. Attributes such as rugal size, shape, density,
428 coverage, and overall tissue keratinization could prove to be informative.

429 *Anatomical Characterization*

430 While viscosity perception in the oral cavity is more multifaceted than originally
431 hypothesized, anatomical characterization does appear to suggest that the perception of high-
432 viscosity solutions on the tongue is related to the filiform papillary attributes of length and
433 density (Figure 6A and B). Moreover, causal analysis finds that variation in PB JND is
434 sufficiently explained by these papillary attributes alone (Table 1). Papillary length appears to be
435 the most relevant attribute and can also serve to explain individuals with unusually high or low
436 JNDs for their density (See ↓ and * in Figure 6A and B). Though these individuals had
437 approximately equivalent papillary densities (8, * vs 8.38, ↓), ↓ had a much higher JND than
438 anticipated (JND = 3874.63cP), while * had a much lower one (JND = 488.00cP). When looking
439 at the length for these individuals the cause of their extreme nature becomes apparent. ↓ had a
440 very short average papillary length (Avg. length = 462.95μm), while * had a much higher
441 average (Avg. length = 905.24μm). This points to the idea that density may not be relevant when
442 structures are too squat to deform or, if innervation is below and not within the papillae,
443 potentially too small to generate sufficient strain on the tongue's surface for signal transduction.
444 Similarly, if structures are long enough, the converse is likely true. This confirmation of the
445 mechanosensory relevance of these structures in viscosity points to their potential relevance in
446 other textural percepts.

447 It is also important to note that sample analysis via optical profiling also indicated a
448 larger degree of variance in papillary shape and size than originally suggested (Figure 4A-D and
449 Figure 5A-C). While values were not as low as the 250μm proposed in the modelling papers,

450 structures ranged in average length by over 600 μ m (Figure 4A-D) [8,9]. This degree of variation
451 present may explain the inconsistencies in the values previously reported in anatomical studies
452 [12,13]. Additionally, there does not appear to be a specific, optimal papillary geometry that is
453 more or less sensitive to these viscosity differences. However, future investigation into additional
454 papillary attributes including hair-like projection length and number, as well as overall papillary
455 rigidity may provide further insight into this mechanism.

456

457 **Conclusions**

458 Findings from this study serve to confirm an idea previously only suggested theoretically:
459 the perception of high-viscosity solutions on the tongue involves the deformation of the filiform
460 papillae. However, findings also serve to highlight the fact that the tongue is not the sole
461 structure involved in oral viscosity perception. Instead, the palate and tongue are playing
462 approximately equal roles generally, while at an individual level there is a differential utilization
463 of the tongue and palate when discriminating between high-viscosity solutions. It is even
464 possible that individuals may be able to overcome a lack of sensitivity in one tissue by
465 compensating with the other.

466

467 **Acknowledgements**

468 The author would like to thank Tabitha Herron from the Department of Oral and
469 Maxillofacial Surgery for her assistance coordinating and scheduling biopsies for test
470 participants. Research support was provided by state and federal funds appropriated to The Ohio
471 State University, Ohio Agricultural Research and Development Center.

472

473 **References**

- 474 [1] P. Haggard, L. De Boer, Neuroscience and biobehavioral reviews oral somatosensory
 475 awareness, *Neurosci. Biobehav. Rev.* 47 (2014) 469–484.
 476 Doi:10.1016/j.neubiorev.2014.09.015.
- 477 [2] C.M. Christensen, L.M. Casper, Oral and nonoral perception of solution viscosity, *J. Food*
 478 *Sci.* 52 (1987) 445–447. Doi:10.1111/j.1365-2621.1987.tb06635.x.
- 479 [3] F. Shama, C. Parkinson, P. Sherman, Identification of stimuli controlling the sensory
 480 evaluation of viscosity in oral methods, *J. Texture stud.* 4 (1973) 102–110.
 481 Doi:10.1111/j.1745-4603.1973.tb00656.x.
- 482 [4] C.H. Smith, J.A. Logemann, W.R. Burghardt, S.G. Zecker, A.W. Rademaker, Oral and
 483 oropharyngeal perceptions of fluid viscosity across the age span, *Dysphagia.* 21 (2006)
 484 209–217. Doi:10.1007/s00455-006-9045-4.
- 485 [5] C.M. Christensen, Perception of solution viscosity, *J. Texture stud.* 10 (1979) 1–8.
- 486 [6] C.M. Steele, D.F. James, S. Hori, R.C. Polacco, C. Yee, Oral perceptual discrimination of
 487 viscosity differences for non-newtonian liquids in the nectar- and honey-thick ranges,
 488 *Dysphagia.* 29 (2014) 355–364. Doi:10.1007/s00455-014-9518-9.
- 489 [7] C.C. Elejalde, J.L. Kokini, The psychophysics of pouring, spreading and in-mouth
 490 viscosity, *J. Texture Stud.* 23 (1992) 315–336. Doi:10.1111/j.1745-4603.1992.tb00528.x.
- 491 [8] G. A. Van Aken, Modelling texture perception by soft epithelial surfaces, *Soft Matter.* 6
 492 (2010) 826. Doi:10.1039/b916708k.
- 493 [9] E. Lauga, C.J. Pipe, B. Le Révérend, Sensing in the mouth: a model for filiform papillae
 494 as strain amplifiers, *Front. Phys.* 4 (2016) 1–8. Doi:10.3389/fphy.2016.00035.
- 495 [10] A.C. Noel, D.L. Hu, The tongue as a gripper, *J. Exp. Biol.* 221 (2018).
 496 Doi:10.1242/jeb.176289.
- 497 [11] M. Manabe, H.W. Lim, M. Winzer, C.A. Loomis, Architectural organization of filiform
 498 papillae in normal and black hairy tongue epithelium: dissection of differentiation
 499 pathways in a complex human epithelium according to their patterns of keratin
 500 expression., *Arch. Dermatol.* 135 (1999) 177–81. Doi:10.1001/archderm.135.2.177.
- 501 [12] K. Kobayashi, M. Kumakura, H. Shinkai, K. Ishii, Three-dimensional fine structure of the
 502 lingual papillae and their connective tissue cores in the human tongue, *Acta Anat. Nippon.*
 503 69 (1994) 624–635. Doi:10.2214/ajr.09.3938.
- 504 [13] A. Kulla-Mikkonen, T.E. Sorvari, A scanning electron microscopic study of the dorsal
 505 surface of the human tongue, *Acta Anat.* 123 (1985) 114–120.
- 506 [14] C.M. Steele, W.A. Alsanei, S. Ayanikalath, C.E.A. Barbon, J. Chen, J.A.Y. Cichero, K.
 507 Coutts, R.O. Dantas, J. Duivesteyn, L. Giosa, B. Hanson, P. Lam, C. Lecko, C. Leigh, A.
 508 Nagy, A.M. Namasivayam, W. V. Nascimento, I. Odendaal, C.H. Smith, H. Wang, The
 509 influence of food texture and liquid consistency modification on swallowing physiology
 510 and function: a systematic review, *Dysphagia.* 30 (2015) 2–26. Doi:10.1007/s00455-014-
 511 9578-x.
- 512 [15] A.N. Cutler, E.R. Morris, L.J. Taylor, Oral perception of viscosity in fluid foods and
 513 model systems, *J. Tex.* 14 (1983) 377–395.
- 514 [16] T.M. Nuessle, N.L. Garneau, M.M. Sloan, S.A. Santorico, Denver papillae protocol for
 515 objective analysis of fungiform papillae, *J. Vis. Exp.* 100 (2015) 1–9. Doi:10.3791/52860.
- 516 [17] W.J. Hume, C.S. Potten, The ordered columnar structure of mouse filiform papillae, *J.*
 517 *Cell Sci.* 22 (1976) 149–160.

- 518 [18] S. Iwasaki, H. Yoshizawa, I. Kawahara, Study by scanning electron microscopy of the
519 morphogenesis of three types of lingual papillae in the mouse, *Acta Anat.* 157 (1996) 41–
520 52.
- 521 [19] R.G. Bangcuyo, C.T. Simons, Lingual tactile sensitivity: effect of age group, sex, and
522 fungiform papillae density, *Exp. Brain Res.* 235 (2017) 2679–2688. Doi:10.1007/s00221-
523 017-5003-7.
- 524 [20] C.M. Steele, L. Hill, S. Stokely, M. Peladeau-Pigeon, Age and strength influences on
525 lingual tactile acuity, *J. Texture Stud.* 45 (2014) 317–323.
526 Doi:10.3174/ajnr.a1256.functional.
- 527 [21] B. Linne, C.T. Simons, Quantification of oral roughness perception and comparison with
528 mechanism of astringency perception, *Chem. Senses.* 42 (2017) 525–535.
529 Doi:10.1093/chemse/bjx029.
- 530 [22] B.L. Miles, K. Van Simaey, M. Whitecotton, C.T. Simons, Comparative tactile
531 sensitivity of the fingertip and apical tongue using complex and pure tactile tasks, *Physiol.*
532 *Behav.* (2018). Doi:10.1016/j.physbeh.2018.07.002.
- 533 [23] X.H. Yang, W.L. Zhu, Viscosity properties of sodium carboxymethylcellulose solutions,
534 *Cellulose.* 14 (2007) 409–417. Doi:10.1007/s10570-007-9137-9.
- 535 [24] L. Engelen, A. Van Der Bilt, M. Schipper, F. Bosman, Oral size perception of particles:
536 effect of size, type, viscosity and method, *J. Texture Stud.* 36 (2005) 373–386.
537 Doi:10.1111/j.1745-4603.2005.00022.x.
- 538 [25] D.R. Risky, J.A. Desor, D. Vellucci, Effects of gymnemic acid concentration and time
539 since exposure on intensity of simple tastes: a test of the biphasic model for the action of
540 gymnemic acid, *Chem. Senses.* 7 (1982) 143–152. Doi:10.1093/chemse/7.2.143.
- 541 [26] L. Engelen, J.F. Prinz, F. Bosman, The influence of density and material on oral
542 perception of ball size with and without palatal coverage, *Arch. Oral Biol.* 47 (2002) 197–
543 201. Doi:10.1016/s0003-9969(01)00106-6.
- 544 [27] Y. Moayedi, L.F. Duenas-Bianchi, E.A. Lumpkin, Somatosensory innervation of the oral
545 mucosa of adult and aging mice, *Nat. Sci. Reports.* 8 (2018) 1–14. Doi:10.1038/s41598-
546 018-28195-2.
- 547